

World Journal of *Gastroenterology*

World J Gastroenterol 2024 February 14; 30(6): 516-613



EDITORIAL

- 516 Diagnostic tools for fecal incontinence: Scoring systems are the crucial first step
Liptak P, Duricek M, Banovcin P
- 523 Unmet needs in biomarkers for autoimmune pancreatitis diagnosis
Wang BC, Fan JG

REVIEW

- 527 Emerging role of exosomes in ulcerative colitis: Targeting NOD-like receptor family pyrin domain containing 3 inflammasome
Li X, Ji LJ, Feng KD, Huang H, Liang MR, Cheng SJ, Meng XD

ORIGINAL ARTICLE**Retrospective Study**

- 542 Preoperative prediction of lymphovascular and perineural invasion in gastric cancer using spectral computed tomography imaging and machine learning
Ge HT, Chen JW, Wang LL, Zou TX, Zheng B, Liu YF, Xue YJ, Lin WW

Clinical Trials Study

- 556 Optimized sequential therapy *vs* 10- and 14-d concomitant therapy for eradicating *Helicobacter pylori*: A randomized clinical trial
Seddik H, Benass J, Berrag S, Sair A, Berraida R, Boutallaka H

Basic Study

- 565 Role of deubiquitinase JOSD2 in the pathogenesis of esophageal squamous cell carcinoma
Wang WP, Shi D, Yun D, Hu J, Wang JF, Liu J, Yang YP, Li MR, Wang JF, Kong DL

META-ANALYSIS

- 579 Urea breath test for *Helicobacter pylori* infection in adult dyspeptic patients: A meta-analysis of diagnostic test accuracy
Lemos FFB, Castro CT, Silva Luz M, Rocha GR, Correa Santos GL, de Oliveira Silva LG, Calmon MS, Souza CL, Zarpelon-Schutz AC, Teixeira KN, Queiroz DMM, Freire de Melo F

CASE REPORT

- 599 Y-Z deformable magnetic ring for the treatment of rectal stricture: A case report and review of literature
Zhang MM, Sha HC, Qin YF, Lyu Y, Yan XP

LETTER TO THE EDITOR

- 607** Angiotensin-converting enzyme 2 alleviates liver fibrosis through the renin-angiotensin system
Zhao BW, Chen YJ, Zhang RP, Chen YM, Huang BW
- 610** Endoscopic intramural cystogastrostomy for treatment of peripancreatic fluid collection: A viewpoint from a surgeon
Ker CG

ABOUT COVER

Editorial Board Member of *World Journal of Gastroenterology*, Kok Yang Tan, FRCS (Ed), MBBS, Associate Professor, Chief Doctor, Senior Lecturer, Surgeon, Department of Surgery, Khoo Teck Puat Hospital, Singapore 768828, Singapore. kokyangtan@gmail.com

AIMS AND SCOPE

The primary aim of *World Journal of Gastroenterology* (*WJG*, *World J Gastroenterol*) is to provide scholars and readers from various fields of gastroenterology and hepatology with a platform to publish high-quality basic and clinical research articles and communicate their research findings online. *WJG* mainly publishes articles reporting research results and findings obtained in the field of gastroenterology and hepatology and covering a wide range of topics including gastroenterology, hepatology, gastrointestinal endoscopy, gastrointestinal surgery, gastrointestinal oncology, and pediatric gastroenterology.

INDEXING/ABSTRACTING

The *WJG* is now abstracted and indexed in Science Citation Index Expanded (SCIE), MEDLINE, PubMed, PubMed Central, Scopus, Reference Citation Analysis, China Science and Technology Journal Database, and Superstar Journals Database. The 2023 edition of Journal Citation Reports® cites the 2022 impact factor (IF) for *WJG* as 4.3; Quartile category: Q2. The *WJG*'s CiteScore for 2021 is 8.3.

RESPONSIBLE EDITORS FOR THIS ISSUE

Production Editor: *Ying-Yi Yuan*; Production Department Director: *Xiang Li*; Editorial Office Director: *Jia-Ru Fan*.

NAME OF JOURNAL

World Journal of Gastroenterology

ISSN

ISSN 1007-9327 (print) ISSN 2219-2840 (online)

LAUNCH DATE

October 1, 1995

FREQUENCY

Weekly

EDITORS-IN-CHIEF

Andrzej S Tarnawski

EXECUTIVE ASSOCIATE EDITORS-IN-CHIEF

Xian-Jun Yu (Pancreatic Oncology), Jian-Gao Fan (Chronic Liver Disease), Hou-Bao Liu (Biliary Tract Disease)

EDITORIAL BOARD MEMBERS

<http://www.wjgnet.com/1007-9327/editorialboard.htm>

PUBLICATION DATE

February 14, 2024

COPYRIGHT

© 2024 Baishideng Publishing Group Inc

PUBLISHING PARTNER

Shanghai Pancreatic Cancer Institute and Pancreatic Cancer Institute, Fudan University
Biliary Tract Disease Institute, Fudan University

INSTRUCTIONS TO AUTHORS

<https://www.wjgnet.com/bpg/gerinfo/204>

GUIDELINES FOR ETHICS DOCUMENTS

<https://www.wjgnet.com/bpg/GerInfo/287>

GUIDELINES FOR NON-NATIVE SPEAKERS OF ENGLISH

<https://www.wjgnet.com/bpg/gerinfo/240>

PUBLICATION ETHICS

<https://www.wjgnet.com/bpg/GerInfo/288>

PUBLICATION MISCONDUCT

<https://www.wjgnet.com/bpg/gerinfo/208>

POLICY OF CO-AUTHORS

<https://www.wjgnet.com/bpg/GerInfo/310>

ARTICLE PROCESSING CHARGE

<https://www.wjgnet.com/bpg/gerinfo/242>

STEPS FOR SUBMITTING MANUSCRIPTS

<https://www.wjgnet.com/bpg/GerInfo/239>

ONLINE SUBMISSION

<https://www.f6publishing.com>

PUBLISHING PARTNER'S OFFICIAL WEBSITE

<https://www.shca.org.cn>
<https://www.zs-hospital.sh.cn>

Retrospective Study

Preoperative prediction of lymphovascular and perineural invasion in gastric cancer using spectral computed tomography imaging and machine learning

Hui-Ting Ge, Jian-Wu Chen, Li-Li Wang, Tian-Xiu Zou, Bin Zheng, Yuan-Fen Liu, Yun-Jing Xue, Wei-Wen Lin

Specialty type: Gastroenterology and hepatology

Provenance and peer review: Invited article; Externally peer reviewed.

Peer-review model: Single blind

Peer-review report's scientific quality classification

Grade A (Excellent): 0
Grade B (Very good): B
Grade C (Good): 0
Grade D (Fair): 0
Grade E (Poor): 0

P-Reviewer: Osera S, Japan

Received: October 20, 2023

Peer-review started: October 20, 2023

First decision: December 5, 2023

Revised: December 18, 2023

Accepted: January 15, 2024

Article in press: January 15, 2024

Published online: February 14, 2024



Hui-Ting Ge, Tian-Xiu Zou, Yuan-Fen Liu, Yun-Jing Xue, Wei-Wen Lin, Department of Radiology, Fujian Medical University Union Hospital, Fuzhou 350001, Fujian Province, China

Hui-Ting Ge, Jian-Wu Chen, Li-Li Wang, Fujian Key Laboratory of Intelligent Imaging and Precision Radiotherapy for Tumors, Fujian Medical University, Fuzhou 350001, Fujian Province, China

Hui-Ting Ge, Jian-Wu Chen, Li-Li Wang, Digestive, Hematological and Breast Malignancies, Clinical Research Center for Radiology and Radiotherapy of Fujian Province, Fuzhou 350001, Fujian Province, China

Jian-Wu Chen, Department of Radiation Oncology, Fujian Medical University Union Hospital, Fuzhou 350001, Fujian Province, China

Li-Li Wang, Department of Diagnostic Radiology, Fujian Medical University Union Hospital, Fuzhou 350001, Fujian Province, China

Bin Zheng, School of Electrical and Computer Engineering, University of Oklahoma, Oklahoma, OK 73019, United States

Corresponding author: Wei-Wen Lin, PhD, Doctor, Professor, Researcher, Department of Radiology, Fujian Medical University Union Hospital, Xinquan Road, Gulou District, Fuzhou 350001, Fujian Province, China. wwl152559063@163.com

Abstract

BACKGROUND

Lymphovascular invasion (LVI) and perineural invasion (PNI) are important prognostic factors for gastric cancer (GC) that indicate an increased risk of metastasis and poor outcomes. Accurate preoperative prediction of LVI/PNI status could help clinicians identify high-risk patients and guide treatment decisions. However, prior models using conventional computed tomography (CT) images to predict LVI or PNI separately have had limited accuracy. Spectral CT provides quantitative enhancement parameters that may better capture tumor invasion. We hypothesized that a predictive model combining clinical and spectral CT parameters would accurately preoperatively predict LVI/PNI status in GC patients.

AIM

To develop and test a machine learning model that fuses spectral CT parameters and clinical indicators to predict LVI/PNI status accurately.

METHODS

This study used a retrospective dataset involving 257 GC patients (training cohort, $n = 172$; validation cohort, $n = 85$). First, several clinical indicators, including serum tumor markers, CT-TN stages and CT-detected extramural vein invasion (CT-EMVI), were extracted, as were quantitative spectral CT parameters from the delineated tumor regions. Next, a two-step feature selection approach using correlation-based methods and information gain ranking inside a 10-fold cross-validation loop was utilized to select informative clinical and spectral CT parameters. A logistic regression (LR)-based nomogram model was subsequently constructed to predict LVI/PNI status, and its performance was evaluated using the area under the receiver operating characteristic curve (AUC).

RESULTS

In both the training and validation cohorts, CT T3-4 stage, CT-N positive status, and CT-EMVI positive status are more prevalent in the LVI/PNI-positive group and these differences are statistically significant ($P < 0.05$). LR analysis of the training group showed preoperative CT-T stage, CT-EMVI, single-energy CT values of 70 keV of venous phase (VP-70 keV), and the ratio of standardized iodine concentration of equilibrium phase (EP-NIC) were independent influencing factors. The AUCs of VP-70 keV and EP-NIC were 0.888 and 0.824, respectively, which were slightly greater than those of CT-T and CT-EMVI (AUC = 0.793, 0.762). The nomogram combining CT-T stage, CT-EMVI, VP-70 keV and EP-NIC yielded AUCs of 0.918 (0.866-0.954) and 0.874 (0.784-0.936) in the training and validation cohorts, which are significantly higher than using each of single independent factors ($P < 0.05$).

CONCLUSION

The study found that using portal venous and EP spectral CT parameters allows effective preoperative detection of LVI/PNI in GC, with accuracy boosted by integrating clinical markers.

Key Words: Spectral computed tomography; Gastric cancer; Lymphovascular invasion; Perineural invasion

©The Author(s) 2024. Published by Baishideng Publishing Group Inc. All rights reserved.

Core Tip: This study developed a machine learning model using clinical indicators and spectral computed tomography (CT) imaging parameters to preoperatively predict lymphovascular and perineural invasive risk in gastric cancer patients. The model combining CT staging, extramural vein invasive based on CT, and quantitative spectral CT measures had high accuracy for noninvasive prediction of these important histological features.

Citation: Ge HT, Chen JW, Wang LL, Zou TX, Zheng B, Liu YF, Xue YJ, Lin WW. Preoperative prediction of lymphovascular and perineural invasion in gastric cancer using spectral computed tomography imaging and machine learning. *World J Gastroenterol* 2024; 30(6): 542-555

URL: <https://www.wjgnet.com/1007-9327/full/v30/i6/542.htm>

DOI: <https://dx.doi.org/10.3748/wjg.v30.i6.542>

INTRODUCTION

Currently, gastric cancer (GC) ranks fifth in global cancer incidence and fourth in mortality[1]. Accurate preoperative evaluation of GC stage and tumor invasiveness is important for developing personalized treatment. In GC development, nerves, blood vessels, and lymphatic connections constitute the tumor microenvironment, and cancer cells can spread throughout the body by invading lymphatic blood vessels, and nerve fiber sheaths. Therefore, lymphovascular invasion (LVI) and perineural invasion (PNI) are closely related to tumor stage, depth of invasion, lymphatic metastasis, and distant metastasis in GC patients. As a result, the LVI and PNI can be used to predict tumor invasion and patient prognosis (or patient response to treatment)[2-4]. Previous studies have shown that a positive LVI/PNI can be used as an indicator of the efficacy of neoadjuvant and adjuvant therapies in GC patients[5,6]. At present, LVI/PNI can be diagnosed or determined only by postoperative pathology. Therefore, preoperative assessment of LVI and the PNI may assist oncologists in preoperatively identifying high-risk categories and predicting outcomes in GC patients.

In addition to postoperative pathology methods, other diagnostic methods have been identified. For example, one previous study showed a correlation among gastric wall invasion, lymph node metastasis, and the PNI[7]. Chen *et al*[8] reported that clinical T staging, N staging, American Joint Committee on Cancer (AJCC) staging, and enhanced computed tomography (CT) radiomics could be used to predict LVI. Yardımcı *et al*[9] confirmed that machine learning-based CT texture analysis was more successful at predicting LVI than was the PNI. However, these studies were usually based on conventional CT images used to construct models to predict LVI status or PNI status separately.

As a new scanning mode, spectral CT imaging has a variety of quantitative parameters, which enables CT imaging to enter the field of microscopic quantitative research from macroscopic morphology[10]. Previous studies have proven that the quantitative assessment of spectral CT image parameters could be used to evaluate the histological classification, staging, lymph node metastasis, and prognosis of GC patients[11-13]. Ren *et al* showed that cancer antigen 125 (CA125) levels, histological grade, Borrmann grade and energy-based spectrum CT parameters could be used to evaluate LVI and the PNI[14]. However, these studies need further validation. To our knowledge, few studies have focused on assessing the value of using spectral CT imaging and machine learning algorithms to predict LVI and PNI in GC patients preoperatively.

To better address this clinical issue, we hypothesized that optimal fusion of spectral CT parameters and clinical markers using a machine learning method could more accurately predict LVI or PNI status in GC patients preoperatively. Thus, the objective of this study is to test our hypothesis. Specifically, we first used a logistic regression (LR) method to analyze a number of important clinical indicators, including preoperative CT evaluation of gastric wall invasion depth (CT-T stage), lymph node metastasis (CT-N stage), CT-detected extramural vein invasion (CT-EMVI), and serum tumor markers, as well as quantitative spectral CT parameters, and then build a LR-based nomogram model that optimally fuses quantitative spectral CT parameters and clinical indicators (or markers), to predict histological LVI and PNI statuses in GC.

MATERIALS AND METHODS

Patients

This was a retrospective study in which we selected data from patients with gastric adenocarcinoma who underwent surgical resection and were pathologically diagnosed from December 2017 to June 2023 in our hospital. The inclusion criteria are as follows: (1) Diagnosis of gastric adenocarcinoma with clear LVI and PNI information; (2) Abdominal three-phase enhanced spectral CT scan performed within 2 wk before surgery; and (3) No local or systemic treatment performed before CT examination or surgery. The exclusion criteria were as follows: (1) Unclear lesion on CT image; (2) Poor gastric filling, (3) Poor image quality; and (4) Incomplete clinical information. Using the above criteria, the clinical information and preoperative spectral CT images of 257 patients were obtained in this study. According to the postoperative pathological results, patients with LVI and/or PNI were classified as the positive group (LVI/PNI positive, $n = 162$), and patients without LVI and PNI were classified as the negative group (LVI/PNI negative, $n = 95$), as shown in Figure 1.

Clinical information

Clinical data, including sex, age, serum tumor marker levels, and pathological information, were collected by a senior attending physician. The serum tumor markers included CA72-4, alfa fetoprotein (AFP), carcinoembryonic antigen (CEA), CA19-9 and CA125. The pathological information included histological type and complete LVI and PNI data.

CT examination

All preoperative CT images were acquired using a GE Healthcare Revolution CT ascending spectral scanner. Before examination, all patients were asked to fast for 8 h and drink 800-1000 mL of water. The acquisition parameters were as follows: (1) Scanning range; (2) Mid-upper abdomen; (3) Tube voltage, 80 kVp to 140 kVp instantaneous switch; (4) Tube current, 200 mAs; (5) Width of detector, 80 mm; (6) Pitch, 0.992:1; (7) Speed, 0.6-0.8 s/revolution; and (8) Image matrix, 512 × 512. A single-energy image at 70 keV was reconstructed with an image slice thickness of 1.25 mm. Before CT examination, a nonionic water-soluble contrast agent (Dimyron 400 mg/mL, Shanghai Bracco Sine Pharmaceutical Corp. Ltd.) used was injected through the cubital vein of the patient with a high-pressure syringe. The dose was 1.5 mL/kg, and the injection rate was 2.5-3 mL/s. Images in the arterial phase (AP), portal venous phase (VP) and equilibrium phase (EP) were scanned at 20-25 s, 60 s, and 3 min after the start of contrast medium injection.

Imaging analysis

First, two senior attending radiologists (with 7 and 13 years of experience in abdominal radiology, respectively) were blinded to the clinical information and independently and retrospectively reviewed the CT images. All TN stages and EMVIs were evaluated on multiplanar reconstruction images constructed using an AW4.6 workstation. The TN staging and EMVI scores were assigned based on the consensus between the two radiologists. Any discrepancies were resolved by a third senior radiologist (with 32 years of experience in abdominal radiology).

TN staging was performed on the CT images according to the 7th edition of AJCC guidelines and the study by Kim *et al* [15]. CT-EMVI was defined and scored based on the criteria outlined by Yang *et al*[16]. A positive CT-EMVI was defined as a GC lesion directly invading the extramural vascular lumen, resulting in vascular dilation or filling defects, and connecting with the primary tumor mass. EMVI scores of 0-2 and 3-4 are considered negative, and positive CT-EMVI, respectively. The CT-EMVI scoring criteria are described below Figure 2.

Quantitative image analysis was performed on a GE AW4.6 workstation using GSI Viewer software, as depicted in Figure 3. An experienced abdominal radiologist (7 years) who was blinded to the clinical data delineated circular or elliptical regions of interests (ROIs) on the largest cross-sectional area of each tumor, encompassing approximately two-thirds of the lesion volume while avoiding necrotic regions. Each lesion ROI was measured three times, and the average values were calculated. The following spectral CT parameters across three contrast phases were obtained including: (1) Single-energy CT values of 40 keV, 70 keV, 120 keV and 140 keV; (2) Iodine concentration (IC); and (3) Effective atomic

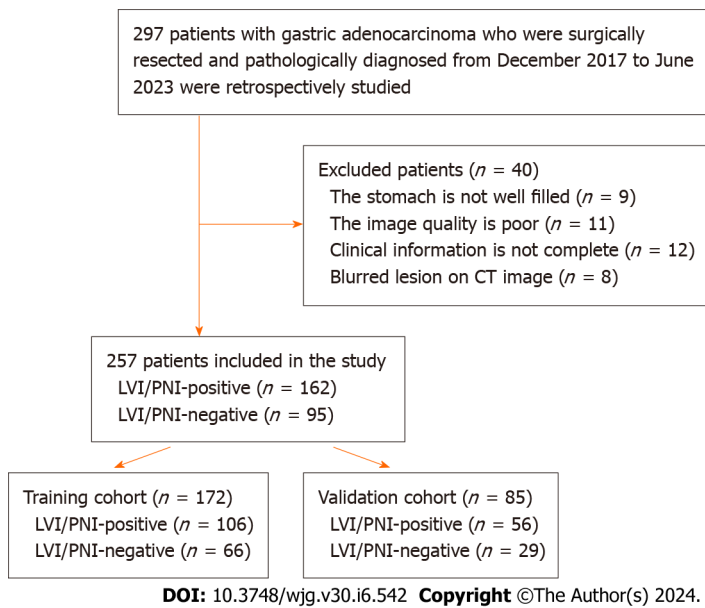


Figure 1 Flowchart of the inclusion and exclusion criteria. LVI: Lymphovascular invasion; PNI: Perineural invasion; CT: Computed tomography.

number (Zeff). Two additional metrics were also derived, namely: (1) The spectral curve slope, calculated as $K_{40-70} = (CT_{40\text{ keV}} - CT_{70\text{ keV}}) / 30$; and (2) The normalized IC ratio (NIC), defined as the lesion IC divided by the thoracic aortic IC at the same level. Thus, a total of 24 parameters were extracted and computed from the spectral CT images.

In this study, the inter- and intraclass correlation coefficients (ICCs) were also calculated to assess the reproducibility of the spectral CT parameters extracted from the ROIs delineated by two radiologists. Radiologist A, who has 7 years of experience, first completed the ROI outlines for all the patients. Radiologist B, who has 13 years of experience, independently outlined the ROIs for a randomly selected subset of 50 patients to evaluate interobserver agreement. Radiologist A also repeated the ROI outlines for the same 50 patients after one month to allow assessment of intraobserver agreement. Spectral CT parameters with ICC values ≥ 0.75 were considered adequately reproducible and were retained for further analysis.

Feature engineering

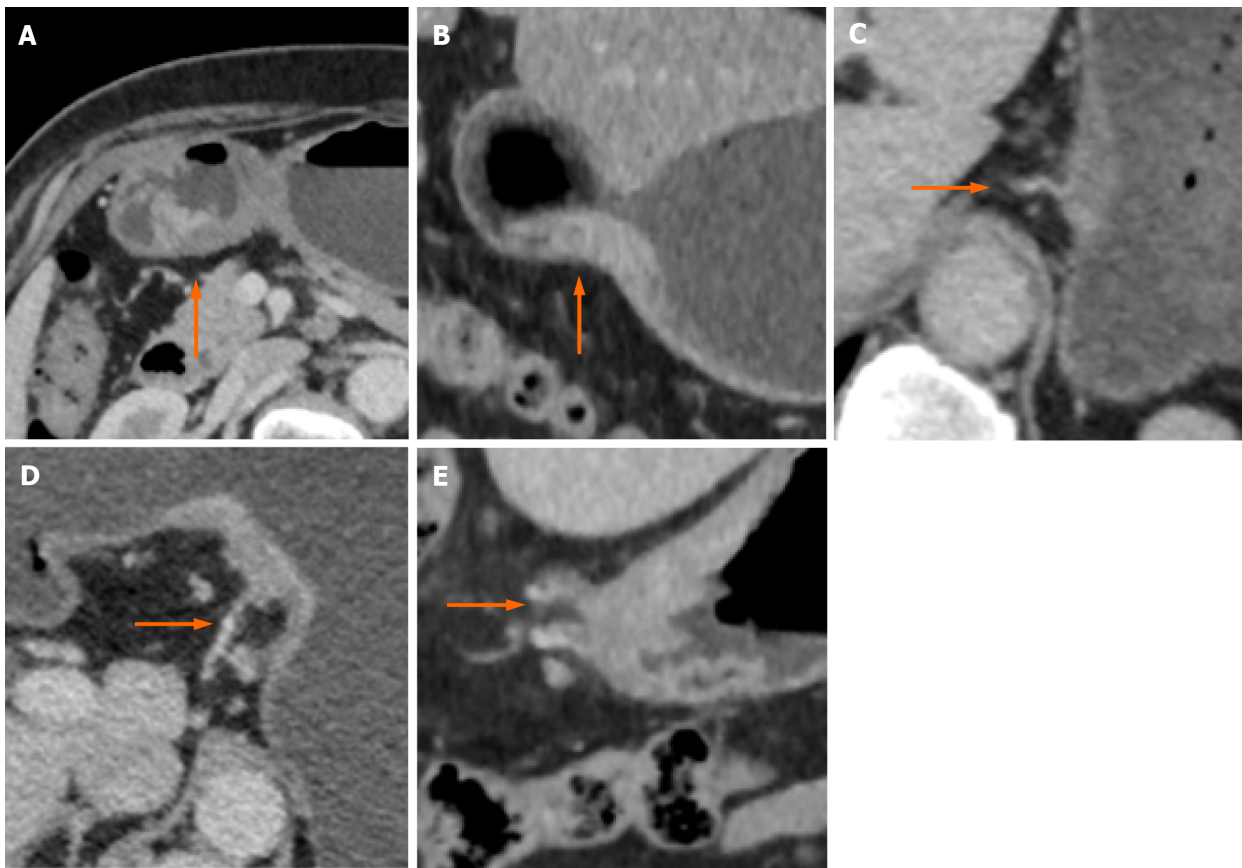
Figure 4 outlines the steps of computing, selecting features, building a machine learning model and evaluating model performance. First, a total of 257 patients diagnosed with GC were divided into the original in the training cohort ($n = 172$) and validation cohort ($n = 85$) in chronological order at a ratio of 2:1. Since 34 features (including 24 spectral CT parameters and 10 clinical indicators) were extracted and computed, some of the features may be redundant. To increase the robustness of the multifeature fusion-based machine learning model, a feature dimensionality reduction step was conducted to select optimal parameters and remove redundant parameters from the whole training cohort *via* the following steps: (1) Univariate analysis was applied to calculate the associations between clinical characteristics and the status of LVI/PNI. Clinical features that showed statistically significant associations were retained for further analysis; and (2) A correlation-based feature selection subset evaluator was used in conjunction with a best-first heuristic feature search and selection method for feature selection. The InfoGainAttributeEval tool was then utilized to evaluate the worth of attributes by measuring their information gain relative to the class. This was paired with a Ranker tool employing a 0.2 average merit threshold for further selection of informative spectral CT parameters. Step 2 was embedded inside a tenfold cross-validation-based iteration cycle to minimize case partition bias, and variance.

A machine learning-based individualized prediction model

Using the selected clinical characteristics and spectral CT parameters, the machine learning algorithm LR was developed using the Akaike information criterion as the stopping criterion. Model performance was evaluated by the area under the receiver operating characteristic curve (AUC) in the training and independent testing cohorts. The Hosmer-Lemeshow test, calibration curves, and bootstrapping (500 resamples) were used to assess model calibration. The AUCs were compared between cohorts *via* DeLong testing. DCA was used to quantify the potential net benefit of the nomogram.

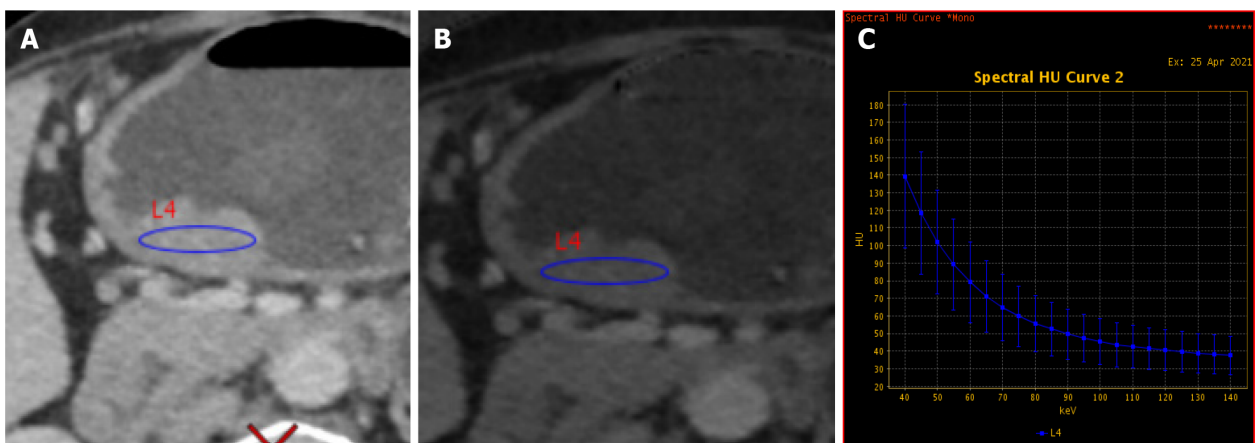
Statistical methods

SPSS 26.0 statistical software was used, and single-factor statistical tests, including the χ^2 test, Fisher's exact test, the Mann-Whitney *U* test and independent sample *t* tests were used. Weka software (version 3.8.6) was used for feature selection, and R software (version 3.4.3) was used for prediction model construction and plotting. $P < 0.05$ was considered to indicate statistical significance.



DOI: 10.3748/wjg.v30.i6.542 Copyright ©The Author(s) 2024.

Figure 2 Example of a computed tomography-detected extramural vein invasion score on computed tomography images of gastric cancer patients. A: Score 0: The tumor has not penetrated the gastric wall, and there are no extramural vessels beside the lesion (arrow) in the transverse position of the venous phase (VP); B: Score 1: The transverse view of the VP shows that the tumor has permeated the gastric wall, and there are no extramural vessels beside the lesion (arrow); C: Score 2: In the VP, the coronal lesion has penetrated the gastric wall, and there are tortuous blood vessels connected with the lesion (arrow), but no tumor density shadow is observed in the vascular lumen; D: Score 3: The transverse view of the VP shows that the mass has penetrated through the gastric wall, the involved blood vessels appear slightly tortuous and dilated, and the tumor density shadow is visible (arrow); E: Score 4: In the coronary view of the VP, the tumor permeated the gastric wall, the extramural vascular lumen was significantly dilated, and a slight low-density filling defect was visible inside (arrow).



DOI: 10.3748/wjg.v30.i6.542 Copyright ©The Author(s) 2024.

Figure 3 Example of the energy spectrum data measurement. A: 70 keV single-energy image; B: The iodine base image; C: The energy spectrum curve. Elliptical regions of interests were drawn at the largest level of the lesion in the lesser curvature of the gastric horn, as shown in A and B.

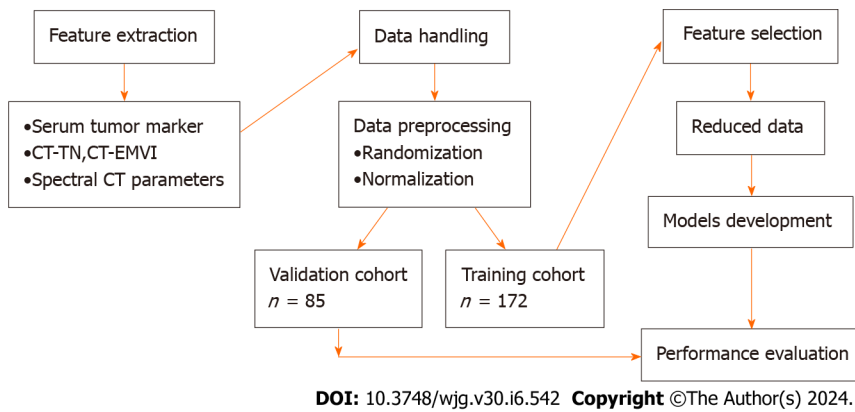


Figure 4 Technical study pipeline. CT-EMVI: Computed tomography-detected extramural vein invasion; CT: Computed tomography.

Comparison of clinical characteristics and quantitative three-phase spectral CT parameters between groups

Figure 5 shows examples of CT and histopathology images of two patients, as well as the energy spectral curves. As shown in Table 1, there were no significant differences between the positive and negative groups in either the training or validation cohorts in terms of sex or age distribution ($P > 0.05$). The data in Table 1 also show the following statistics data analysis results: (1) In both the training and validation cohorts, CT T3-4 stage, CT-N positive status, and CT-EMVI positive status are more prevalent in the LVI/PNI-positive group and these differences are statistically significant ($P < 0.05$); (2) In the training cohort, serum CA72-4 and CA19-9 levels are significantly higher in the LVI/PNI-positive group compared to the LVI/PNI-negative group ($P < 0.05$), however this is not observed in the validation cohort ($P > 0.05$); and (3) There were no significant differences in AFP, CEA, or CA125 levels between the two groups ($P > 0.05$).

The CT values of 40 keV, 70 keV, 120 keV, and 140 keV, K40-70, Zeff, IC, and NIC are higher in the LVI/PNI-positive group compared to the LVI/PNI-negative group at the AP, VP, and EP ($P < 0.05$). The interobserver ICCs for these spectral CT parameters ranged from 0.766 to 0.955, while the intraobserver ICCs ranged from 0.759 to 0.945, indicating good inter- and intraobserver agreement, as all the ICCs exceeded 0.75. These reproducible spectral CT parameters were retained for subsequent feature selection.

Feature selection

After removing 29 redundant features, five features—CT-T stage, CT-N stage, CT-EMVI, single-energy CT values of 70 keV of VP-70 keV, and the ratio of standardized IC of EP (EP-NIC)—were frequently selected by the BestFirst method with $\geq 90\%$ probability. The CT-N stage was then removed after applying InfoGainAttributeEval with a 0.2 average merit threshold. The remaining four features (CT-T stage, CT-EMVI, VP-70 keV CT value, and EP-NIC) were selected and incorporated into LR models. The confusion matrices of clinical and spectral CT features and details of the feature selection process are presented in Tables 1 and 2.

Model performance evaluation

Using training cohort, LR demonstrated that CT-T stage [odds ratio (OR) = 2.683, 95% confidence interval (CI): 1.103-6.523], CT-EMVI (OR = 3.396, 95%CI: 1.277-9.027), VP-70 keV CT value (OR = 1.047, 95%CI: 1.021-1.074), and EP-NIC (OR = 117.723, 95%CI: 4.867-2847.564) were independent influencing factors for predicting LVI/PNI status.

According to the ROC analysis (Table 3 and Figure 6), the AUC of the established LR model was 0.918 (95%CI: 0.866-0.954) in the training cohort, which was greater than that of the single independent factors (0.762-0.888). According to the DeLong tests, the differences between the AUC generated by the LR model and each of the 4 parameters (CT-T, CT-EMVI, VP-70 keV, and EP-NIC) were significant (P values ranging from 0.0428 to 0.0001). A nomogram was constructed for clinical use (Figure 6).

The AUC of the LR model in the validation cohort was 0.874 (95%CI: 0.784-0.936); when each of the 4 parameters was used individually, the AUC ranged from 0.735 to 0.824. There are no significant differences between the paired ROC curves using the same features or LR model applying to the training and validation cohorts with P value > 0.05 , such as $P = 0.3564$ using LR model.

Additionally, the calibration curve and Hosmer-Lemeshow test showed good fit of the nomogram (Figure 6), with no significant differences ($P = 0.6051$). The decision curve analysis confirmed that, compared to the treat-none and treat-all strategies, using the nomogram can help stratify patients based on their predicted risk of LVI/PNI positivity for threshold probabilities between 0.10 and 0.95.

DISCUSSION

This study analyzed quantitative spectral CT parameters, CT-determined TN stage, CT-detected EMVI, and serum tumor markers using a machine learning algorithm. Feature reduction and subsequent LR analysis demonstrated that CT-T stage, CT-EMVI, the VP-70 keV CT value, and the EP-NIC were independent predictors of histological LVI/PNI status.

Table 1 Comparative analysis of clinical indicators and spectral computed tomography parameters between groups

Variables	Training cohort (n = 172)			Validation cohort (n = 85)		
	LVI/PNI (+)	LVI/PNI (-)	P value	LVI/PNI (+)	LVI/PNI (-)	P value
Gender, n (%)						
Male	77 (61.1)	49 (38.9)	0.818	47 (70.2)	20 (29.8)	0.109
Female	29 (63.0)	17 (37.0)		9 (50.0)	9 (50.0)	
Age, yr, n (%)						
< 60	33 (66.0)	17 (34.0)	0.450	19 (67.9)	9 (32.1)	0.788
≥ 60	73 (59.8)	49 (40.2)		37 (64.9)	20 (35.1)	
CT-T						
T1/2	23 (30.3)	53 (69.7)	< 0.001 ^a	9 (28.1)	23 (71.9)	< 0.001 ^a
T3/4	83 (86.5)	13 (13.5)		47 (88.7)	6 (11.3)	
CT-N						
N0	29 (34.9)	54 (65.1)	< 0.001 ^a	19 (55.8)	24 (44.2)	< 0.001 ^a
N1/2/3	77 (86.5)	12 (13.5)		36 (12.2)	5 (87.8)	
CT-EMVI						
Negative	44 (41.5)	62 (58.5)	< 0.001 ^a	20 (45.5)	24 (54.5)	< 0.001 ^a
Positive	62 (6.1)	4 (93.9)		36 (87.8)	5 (12.2)	
CA72-4, n (%)						
Negative	86 (57.3)	64 (42.7)	0.002 ^a	46 (63.9)	26 (36.1)	0.528
Positive	20 (90.9)	2 (9.1)		10 (76.9)	3 (23.1)	
AFP, n (%)						
Negative	104 (61.5)	65 (38.5)	1.000	54 (65.9)	28 (34.1)	1.000
Positive	2 (66.7)	1 (33.3)		2 (66.7)	1 (33.3)	
CEA, n (%)						
Negative	91 (61.1)	58 (38.9)	0.704	42 (61.8)	26 (38.2)	0.109
Positive	15 (65.2)	8 (34.8)		14 (82.4)	3 (17.6)	
CA199, n (%)						
Negative	89 (58.6)	63 (41.4)	0.022 ^a	48 (64.0)	27 (36.0)	0.483
Positive	17 (85.0)	3 (15.0)		8 (80.0)	2 (20.0)	
CA125, n (%)						
Negative	101 (60.5)	66 (39.5)	0.158	54 (65.9)	28 (34.1)	1.000
Positive	5 (100.0)	0 (0.0)		2 (66.7)	1 (33.3)	
VP-70 kev, mean ± SD	92.46 ± 18.29	64.54 ± 15.90	< 0.001 ^a	89.87 ± 20.34	66.30 ± 18.65	< 0.001 ^a
EP-NIC, mean ± SD	0.68 ± 0.16	0.49 ± 0.13	< 0.001 ^a	0.69 ± 0.15	0.51 ± 0.12	< 0.001 ^a

^aP value < 0.05.

P was calculated from univariate association of characteristics with lymphovascular invasion/perineural invasion status in gastric cancer cohorts. LVI: Lymphovascular invasion; PNI: Perineural invasion; (+): Positive; (-): Negative; CT-EMVI: Computed tomography-detected extramural vein invasion; VP-70 keV: Single-energy computed tomography value of 70 keV in the venous phase; EP-NIC: Ratio of the standardized iodine concentration in the equilibrium phase; CA: Cancer antigen; CEA: Carcinoembryonic antigen; AFP: Alfa fetoprotein.

The LR model demonstrated promising results, with comparable accuracy in predicting LVI/PNI across independent training and testing cohorts.

The present study suggested a greater possibility of vascular nerve invasion in the T3-4 stage, which aligns with the findings of previous studies[9] that identified clinical T stage as a predictive factor for LVI. Although CT-determined N status differed significantly according to the χ^2 test, it was removed by the InfoGainAttributeEval tool, which evaluates

Table 2 Risk factors of lymphovascular invasion and perineural invasion in gastric cancer

Variables	Feature selection		Individual nomogram		
	BestFirst with probability (%)	InfoGainAttributeEval with average merit	Z value	OR (95%CI)	P value
CT-EMVI	100	0.203 ± 0.016	2.451	3.396 (1.277-9.027)	0.014
CT-T	100	0.263 ± 0.018	2.177	2.683 (1.103-6.523)	0.029
VP-70kev	90	0.356 ± 0.016	3.565	1.047 (1.021-1.074)	< 0.001
EP-NIC	90	0.239 ± 0.016	2.934	117.723 (4.867-2847.564)	0.003
CT-N	100	0.197 ± 0.014			

CT-EMVI: Computed tomography-detected extramural vein invasion; VP-70 keV: Single-energy computed tomography value of 70 keV in the venous phase; EP-NIC: Ratio of the standardized iodine concentration in the equilibrium phase; OR: Odds ratio; CI: Confidence interval.

Table 3 Performance of the individual nomogram and single independent factors

	AUC (95%CI)	Sensitivity	Specificity	PPV	NPV	Accuracy
Nomogram						
Training cohort	0.918 (0.866-0.954)	85.9	83.3	89.2	78.6	84.9
Validation cohort	0.874 (0.784-0.936)	87.5	75.9	87.5	75.9	83.5
CT-EMVI						
Training cohort	0.762 (0.691-0.824)	58.5	93.9	93.9	58.5	72.1
Validation cohort	0.735 (0.628-0.825)	64.3	82.8	87.8	54.5	70.6
CT-T						
Training cohort	0.793 (0.725-0.851)	78.3	80.3	86.5	69.7	79.1
Validation cohort	0.816 (0.717-0.892)	83.9	79.3	88.7	71.9	82.4
VP-70kev						
Training cohort	0.888 (0.831-0.931)	84.9	71.2	82.6	74.6	79.7
Validation cohort	0.804 (0.703-0.882)	92.9	55.2	80.0	80.0	80.0
EP-NIC						
Training cohort	0.824 (0.758-0.877)	82.1	62.1	77.7	68.3	74.4
Validation cohort	0.824 (0.726-0.898)	85.7	58.6	80.0	68.0	76.5

CT-EMVI: Computed tomography-detected extramural vein invasion; VP-70 keV: Single-energy computed tomography value of 70 keV in the venous phase; EP-NIC: Ratio of the standardized iodine concentration in the equilibrium phase; AUC: Area under the receiver operating characteristic curve; CI: Confidence interval; PPV: Positive predictive value; NPV: Negative predictive value.

attribute worth by measuring information gain relative to the class. This may be because preoperative CT has lower accuracy for N staging than for T staging, as reported previously[17,18].

The presence of an EMVI in CT images is another independent risk factor for LVI/PNI. Previous studies have shown that EMVI usually coexists with invasion of the perigastric nerves, blood vessels, and lymphatic vessels and is considered a route for tumor spread through neurovascular bundles[19]. Our study also confirmed that CT-EMVI is closely related to LVI/PNI status. Patients with positive CT-EMVI findings had a greater probability of having positive LVI/PNI (OR = 3.396, 95%CI: 1.277-9.027).

Serum tumor markers are produced by tumor cells or the body's autoimmune response during tumor growth. CA72-4, AFP, CEA, CA19-9, CA125, and other markers are widely used to diagnose and evaluate the prognosis and treatment efficacy in GC patients[20-22]. Significant differences were found for CA72-4 and CA19-9 in the training cohort ($P < 0.05$) but not in the verification cohort ($P > 0.05$), indicating population-level differences. In contrast, AFP, CEA, and CA125 did not significantly differ ($P > 0.05$). In contrast to our results, Ren *et al*[14] reported higher CA125 levels in LVI/PNI-positive patients. Other studies have shown that GC patients with nerve, vascular, or serosal infiltration and lymph node metastasis have a greater probability of having increased CA72-4[20]. These findings further indicate that serum tumor

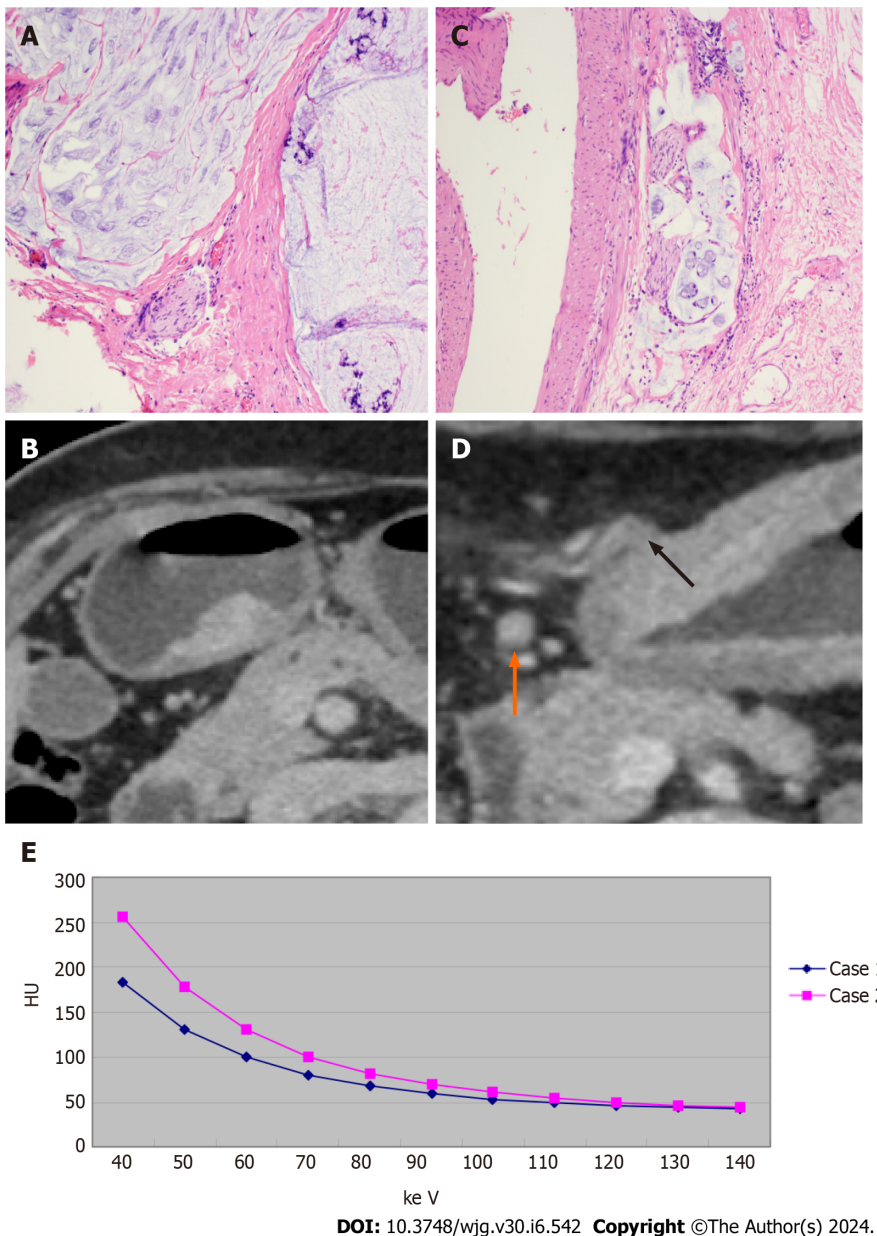


Figure 5 Comparative imaging and spectral analysis of pathological gastric adenocarcinoma in two patients with different lymphovascular and perineural invasion status. A and B: Patient 1: The patient was a 75-year-old female with pathological gastric adenocarcinoma, and both lymphovascular invasion (LVI) and perineural invasion (PNI) were negative (HE, × 200); the equilibrium phase (EP) transverse view shows that the gastric cancer (GC) lesion was immersed in the submucosal low-density layer, and the infiltration depth was more than 50% of the lesion; however, the low-density zone was still visible with an intact outer membrane. No suspicious metastatic lymph nodes were found on the computed tomography (CT) image, and no extramural blood vessels were found around the lesion. The CT stage was CT-T2N0, and CT-detected extramural vein invasion (CT-EMVI) was 0 and negative. The slopes of the energy spectrum curves in the EP were K40-70 = 3.43, IC = 18.46 (100 μg/cm³), normalized iodine concentration (NIC) = 0.40, and effective atomic number (Z_{eff}) = 8.68; C and D: Patient 2: The patient was a 77-year-old male with pathological gastric adenocarcinoma, and both LVI and PNI were positive (HE, × 200). The GC lesion in the transverse position in the equilibrium stage permeated the gastric wall, and a cord-like thickened vascular shadow was observed in the fat space around the lesion. An endovascular low-density filling defect (black arrow) was observed. Enlarged lymph nodes were observed around the lesion, the short diameter was 7 mm (orange arrow), the CT stage was CT-T4aN1, and the CT-EMVI score was 4, indicating positivity. The slopes of the energy spectrum curves in the EP are K40-70 = 5.18, IC = 27.41 (100 μg/cm³), NIC = 0.59, and Z_{eff} = 9.14; E: The energy spectrum curve shows that the CT value at 40-140 keV in patient 2 is greater than that in patient 1, and the value of the slope is greater. The spectral parameters of patient 2 are greater than those of patient 1.

marker levels differ across populations.

The single-energy CT value, IC, and NIC in energy spectrum CT can reflect the degree of blood supply to lesions[23]. Previous studies have indicated that LVI/PNI-positive patients exhibit greater angiogenesis activity and greater microvascular density, resulting in greater lesion enhancement[24]. Therefore, iodine uptake rates (IC and NIC) and single-energy CT values were greater in the positive group than in the negative group. The energy spectrum curve slope and Z_{eff} were also greater in the LVI/PNI-positive group (*P* > 0.05), indicating differences in attenuation characteristics between the groups. An increased lesion mass from the vasculature and endoneurial tumor embolus formation leads to increased Z_{eff}[14].

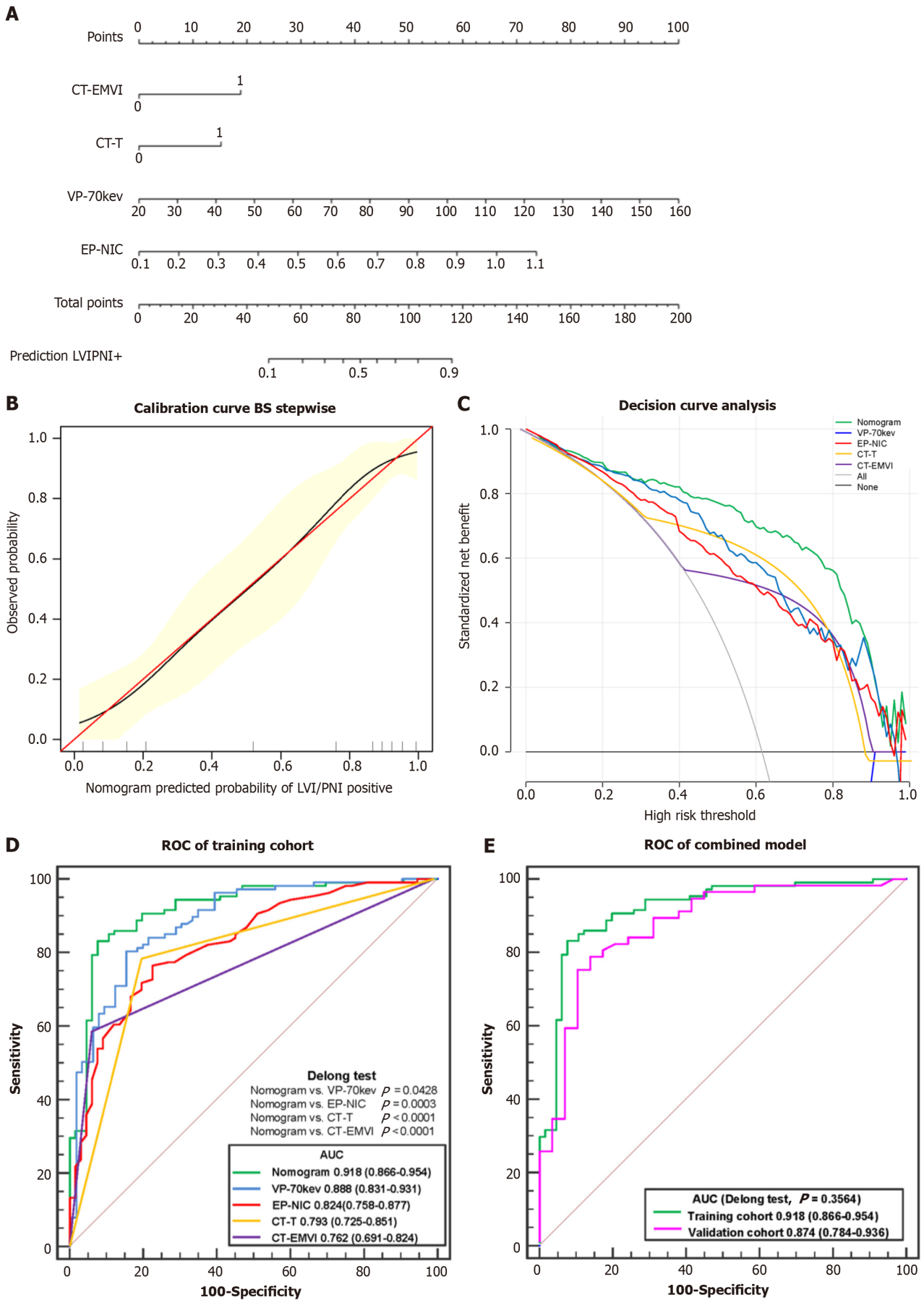


Figure 6 Comprehensive analysis of predictive models. A: Individual nomogram; B: Calibration curve; C: Decision curve analysis of the training cohort; D:

Receiver operating characteristic (ROC) curves of the application of the nomogram, VP-70 keV, EP-NIC, CT-T and CT-EMVI to the training cohort. The DeLong test showed that the differences were significant between the nomogram and each single independent factor; E: ROC curve of the application of the nomogram to the training cohort and the validation cohort. CT-EMVI: Computed tomography-detected extramural vein invasion; VP-70 keV: Single-energy computed tomography value of 70 keV in the venous phase; EP-NIC: Ratio of the standardized iodine concentration in the equilibrium phase; ROC: Receiver operating characteristic; AUC: Area under the receiver operating characteristic curve.

Among the spectral CT quantitative parameters, VP-CT70 keV and EP-NIC were identified as independent predictors of LVI/PNI status by multivariate LR, while arterial-phase parameters were excluded. This may be because the AP mainly reflects intravascular blood supply, whereas the venous and EPs can more effectively reflect blood supply distribution, especially the extracellular lesion space. Thus, venous and EP parameters had better predictive performance than AP parameters. Ren *et al*[14] and Li *et al*[25] also reported superior diagnostic performance for LVI/PNI status using venous-phase spectral parameters. In our study, 70 keV single-energy CT values in the VP were selected as an independent risk factor. This is likely because 70 keV images have the lowest noise, even below that of conventional mixed-energy images, providing the best signal-to-noise ratio[24,26].

Multivariate LR was used to construct predictive models for LVI/PNI status. The AUC of spectral CT quantitative parameters in the venous and EPs for predicting LVI/PNI status was 0.888 and 0.824, respectively, slightly higher than CT-T and CT-EMVI (AUC = 0.793, 0.762). This finding suggested that venous and EP spectral CT alone enables effective assessment. However, the nomogram constructed using combined parameters provides even greater sensitivity and positive predictive value. This allows preoperative identification of high-risk LVI/PNI patients, allowing oncologists to stratify patients into risk categories and adopt more aggressive treatment if warranted. In summary, our study demonstrated the utility of a multiparametric approach using spectral CT for preoperatively identifying high-risk categories and predicting outcomes in GC patients.

This study has several limitations. First, the sample size was relatively small, and there were unequal numbers of patients in the positive and negative LVI/PNI groups. Second, this study focused solely on gastric adenocarcinoma and did not evaluate other histological tumor types. Third, traditional clinicopathological factors were not incorporated into our prediction models. Fourth, as a single-center study, our results may have limited generalizability. Further multicenter studies are warranted to verify the clinical feasibility of implementing these predictive models more broadly.

CONCLUSION

In conclusion, despite these limitations, this study demonstrated the feasibility of using multiphasic spectral CT parameters to preoperatively predict lymphovascular and PNI risk in gastric adenocarcinoma patients. Further validation of this noninvasive approach may enable individualized risk stratification and outcome prediction to optimize treatment.

ARTICLE HIGHLIGHTS

Research background

The research background involves the critical role of lymphovascular invasion (LVI) and perineural invasion (PNI) as prognostic factors in gastric cancer (GC), indicating an increased risk of metastasis and poor patient outcomes. The ability to accurately predict LVI/PNI status preoperatively is significant for identifying high-risk patients and guiding treatment decisions. Conventional models using standard computed tomography (CT) images to predict these invasions have had limited success; thus, this study proposes a new approach using spectral CT imaging and machine learning to improve prediction accuracy.

Research motivation

The research is motivated by the necessity to improve preoperative predictions of LVI and PNI in GC patients, addressing the limitations of conventional CT imaging techniques. The primary objective is to develop a more precise predictive model by integrating spectral CT imaging parameters with clinical markers through machine learning algorithms. Successfully achieving this could refine preoperative assessments, aid in risk stratification, inform treatment planning, and potentially elevate future diagnostic strategies in the field of GC.

Research objectives

The primary objective of the research is to test the hypothesis that an optimal fusion of spectral CT parameters with clinical markers using a machine learning method can more accurately predict LVI or PNI status in GC patients before surgery. Specifically, the study analyzed a set of clinical indicators, such as preoperative CT evaluation of gastric wall invasion depth, lymph node metastasis, extramural vein invasion, and serum tumor markers, along with quantitative spectral CT parameters. The research aimed to develop a logistic regression (LR)-based nomogram model that integrates these clinical indicators with spectral CT parameters to predict histological LVI and PNI statuses in GC. Realizing these objectives has significant implications for improving preoperative staging and tailoring appropriate treatment plans for GC patients, thus advancing future research and diagnostic strategies in this field.

Research methods

The research adopted a retrospective dataset and a LR-based nomogram model that incorporated clinical indicators with quantitative spectral CT parameters for the preoperative prediction of lymphovascular and PNI in GC patients. Methods included using statistical software for univariate analysis and correlation-based feature selection, along with 10-fold cross-validation and information gain ranking within a training-validation cohort framework to select significant features. The model's performance was evaluated through receiver operating characteristic (ROC) analysis, calibration using the Hosmer-Lemeshow test and bootstrapping, and decision curve analysis to quantify potential net benefits. These methods highlighted novel approaches in integrating machine learning with available clinical and imaging data to potentially improve preoperative assessment and treatment planning.

Research results

The research results demonstrated that CT values and parameters such as iodine concentration and normalized iodine concentration were significantly higher in the LVI/PNI-positive group across all phases (arterial, venous, and equilibrium) when compared to the LVI/PNI-negative group, with statistical significance ($P < 0.05$). Good inter- and intra-observer agreement was observed for these spectral CT parameters, as indicated by the inter-observer intraclass correlation coefficients (ICC) values ranging from 0.766 to 0.955 and intra-observer ICC values from 0.759 to 0.945. This reproducibility led to their retention for feature selection in developing the predictive model. These findings contribute to the overall research in the field by introducing reproducible and quantifiable spectral CT parameters as reliable predictors for LVI/PNI status in GC patients. The study opens avenues for further investigation into refining and validating these spectral CT-based assessment methods, possibly addressing existing challenges in preoperative staging and treatment planning.

Research conclusions

The study proposes a novel application of spectral CT imaging integrated with machine learning to preoperatively predict lymphovascular and PNI in patients with GC. Through the use of a logistic regression-based nomogram model, the research introduces a new method for combining clinical indicators with quantitative imaging parameters to improve the accuracy of preoperative assessments. This contributes to the field by proposing an alternative to the current postoperative pathology methods and could improve treatment planning by enabling non-invasive, individualized risk stratification prior to surgery.

Research perspectives

The direction of future research following this study is anticipated to focus on validating the noninvasive spectral CT-based machine learning model in prospective multicenter studies to confirm its clinical utility in preoperative risk stratification. Additionally, further research may explore the integration of this model in routine clinical practice to assess its impact on patient management, particularly in the identification of those who may benefit from more aggressive treatment strategies preoperatively. By refining and expanding the predictive capabilities of spectral CT imaging, future research could pave the way for improved individualized treatment planning and outcomes in GC care.

ACKNOWLEDGEMENTS

We thank all the authors for their contributions to the manuscript and for their recognition of the data and conclusions.

FOOTNOTES

Co-first authors: Hui-Ting Ge and Jian-Wu Chen.

Co-corresponding authors: Yun-Jing Xue and Wei-Wen Lin.

Author contributions: Ge HT, Chen JW, and Wang LL contributed equally to this work; Ge HT, Chen JW, and Wang LL designed the research study and performed the research; Ge HT wrote the manuscript and collected data; Zou TX contributed new software and analytic tools; Wang LL and Zheng B analyzed the data; Liu YF provided methods; Xue YJ and Lin WW searched literature and managed the project; Xue YJ and Lin WW contributed equally to this work; and all authors have read and approve the final manuscript.

Supported by Science and Technology Project of Fujian Province, No. 2022Y0025.

Institutional review board statement: The study was reviewed and approved by the Ethical Review Board of Fujian Medical University Union Hospital (Fuzhou, China), approval No. 2022KJT016.

Informed consent statement: The requirement for informed consent was waived.

Conflict-of-interest statement: All the authors report no relevant conflicts of interest for this article.

Data sharing statement: Technical appendix, statistical code, and dataset available from the corresponding author at ww1152559063@163.com. Participants gave informed consent for data sharing but the presented data are anonymized and risk of identification is low.

Open-Access: This article is an open-access article that was selected by an in-house editor and fully peer-reviewed by external reviewers. It is distributed in accordance with the Creative Commons Attribution NonCommercial (CC BY-NC 4.0) license, which permits others to distribute, remix, adapt, build upon this work non-commercially, and license their derivative works on different terms, provided the original work is properly cited and the use is non-commercial. See: <https://creativecommons.org/licenses/by-nc/4.0/>

Country/Territory of origin: China

ORCID number: Yun-Jing Xue 0000-0003-4563-4763; Wei-Wen Lin 0009-0005-2317-3996.

S-Editor: Wang JJ

L-Editor: A

P-Editor: Zhao YQ

REFERENCES

- Sung H, Ferlay J, Siegel RL, Laversanne M, Soerjomataram I, Jemal A, Bray F. Global Cancer Statistics 2020: GLOBOCAN Estimates of Incidence and Mortality Worldwide for 36 Cancers in 185 Countries. *CA Cancer J Clin* 2021; **71**: 209-249 [PMID: 33538338 DOI: 10.3322/caac.21660]
- Tan X, Yang X, Hu S, Chen X, Sun Z. A nomogram for predicting postoperative complications based on tumor spectral CT parameters and visceral fat area in gastric cancer patients. *Eur J Radiol* 2023; **167**: 111072 [PMID: 37666073 DOI: 10.1016/j.ejrad.2023.111072]
- Hsu CP, Chuang CY, Hsu PK, Chien LI, Lin CH, Yeh YC, Hsu HS, Wu YC. Lymphovascular Invasion as the Major Prognostic Factor in Node-Negative Esophageal Cancer After Primary Esophagectomy. *J Gastrointest Surg* 2020; **24**: 1459-1468 [PMID: 31273552 DOI: 10.1007/s11605-019-04310-0]
- Dobrițoiu M, Stepan AE, Vere CC, Simionescu CE. Evaluation of Gastric Carcinomas Histological Patterns in Relation to Tumors Aggressiveness Parameters. *Curr Health Sci J* 2018; **44**: 342-346 [PMID: 31123609 DOI: 10.12865/CHSJ.44.04.03]
- Ajani JA, D'Amico TA, Almhanna K, Bentrem DJ, Chao J, Das P, Denlinger CS, Fanta P, Farjah F, Fuchs CS, Gerdes H, Gibson M, Glasgow RE, Hayman JA, Hochwald S, Hofstetter WL, Ilson DH, Jaroszewski D, Johung KL, Keswani RN, Kleinberg LR, Korn WM, Leong S, Linn C, Lockhart AC, Ly QP, Mulcahy MF, Orringer MB, Perry KA, Poultsides GA, Scott WJ, Strong VE, Washington MK, Weksler B, Willett CG, Wright CD, Zelman D, McMillian N, Sundar H. Gastric Cancer, Version 3.2016, NCCN Clinical Practice Guidelines in Oncology. *J Natl Compr Canc Netw* 2016; **14**: 1286-1312 [PMID: 27697982 DOI: 10.6004/jnccn.2016.0137]
- Huang ZN, Chen QY, Zheng CH, Li P, Xie JW, Wang JB, Lin JX, Lu J, Cao LL, Lin M, Tu RH, Lin JL, Zheng HL, Huang CM. Are the indications for postoperative radiotherapy in the NCCN guidelines for patients with gastric adenocarcinoma too broad? A study based on the SEER database. *BMC Cancer* 2018; **18**: 1064 [PMID: 30390644 DOI: 10.1186/s12885-018-4957-6]
- Selçukbiricik F, Tural D, Büyükkunal E, Serdengeçti S. Perineural invasion independent prognostic factors in patients with gastric cancer undergoing curative resection. *Asian Pac J Cancer Prev* 2012; **13**: 3149-3152 [PMID: 22994725]
- Chen X, Yang Z, Yang J, Liao Y, Pang P, Fan W, Chen X. Radiomics analysis of contrast-enhanced CT predicts lymphovascular invasion and disease outcome in gastric cancer: a preliminary study. *Cancer Imaging* 2020; **20**: 24 [PMID: 32248822 DOI: 10.1186/s40644-020-00302-5]
- Yardımcı AH, Koçak B, Turan Bektaş C, Sel İ, Yarıkaya E, Dursun N, Bektaş H, Usul Afşar Ç, Gürsu RU, Kılıçkesmez Ö. Tubular gastric adenocarcinoma: machine learning-based CT texture analysis for predicting lymphovascular and perineural invasion. *Diagn Interv Radiol* 2020; **26**: 515-522 [PMID: 32990246 DOI: 10.5152/dir.2020.19507]
- Goo HW, Goo JM. Dual-Energy CT: New Horizon in Medical Imaging. *Korean J Radiol* 2017; **18**: 555-569 [PMID: 28670151 DOI: 10.3348/kjr.2017.18.4.555]
- Li R, Li J, Wang X, Liang P, Gao J. Detection of gastric cancer and its histological type based on iodine concentration in spectral CT. *Cancer Imaging* 2018; **18**: 42 [PMID: 30413174 DOI: 10.1186/s40644-018-0176-2]
- Hong YL, Zhang YS, Ye F, Liu ZJ, Kang JH, Wang JA, Zeng Q. [Value of dual-layer spectral detector CT in preoperative prediction of lymph node metastasis of gastric cancer]. *Zhonghua Yi Xue Za Zhi* 2022; **102**: 1747-1752 [PMID: 35705478 DOI: 10.3760/cma.j.cn112137-20220207-00245]
- Wang R, Li J, Fang MJ, Dong D, Liang P, Gao JB. [The value of spectral CT-based radiomics in preoperative prediction of lymph node metastasis of advanced gastric cancer]. *Zhonghua Yi Xue Za Zhi* 2020; **100**: 1617-1622 [PMID: 32486595 DOI: 10.3760/cma.j.cn112137-20191113-02468]
- Ren T, Zhang W, Li S, Deng L, Xue C, Li Z, Liu S, Sun J, Zhou J. Combination of clinical and spectral-CT parameters for predicting lymphovascular and perineural invasion in gastric cancer. *Diagn Interv Imaging* 2022; **103**: 584-593 [PMID: 35934616 DOI: 10.1016/j.diii.2022.07.004]
- Kim JW, Shin SS, Heo SH, Choi YD, Lim HS, Park YK, Park CH, Jeong YY, Kang HK. Diagnostic performance of 64-section CT using CT gastrography in preoperative T staging of gastric cancer according to 7th edition of AJCC cancer staging manual. *Eur Radiol* 2012; **22**: 654-662 [PMID: 21965037 DOI: 10.1007/s00330-011-2283-3]
- Yang YT, Dong SY, Zhao J, Wang WT, Zeng MS, Rao SX. CT-detected extramural venous invasion is correlated with presence of lymph node metastasis and progression-free survival in gastric cancer. *Br J Radiol* 2020; **93**: 20200673 [PMID: 33002375 DOI: 10.1259/bjr.20200673]
- Wang Y, Liu W, Yu Y, Liu JJ, Xue HD, Qi YF, Lei J, Yu JC, Jin ZY. CT radiomics nomogram for the preoperative prediction of lymph node metastasis in gastric cancer. *Eur Radiol* 2020; **30**: 976-986 [PMID: 31468157 DOI: 10.1007/s00330-019-06398-z]
- Borggreve AS, Goense L, Brenkman HJF, Mook S, Meijer GJ, Wessels FJ, Verheij M, Jansen EPM, van Hillegersberg R, van Rossum PSN, Ruurda JP. Imaging strategies in the management of gastric cancer: current role and future potential of MRI. *Br J Radiol* 2019; **92**: 20181044 [PMID: 30789792 DOI: 10.1259/bjr.20181044]
- Tan CH, Vikram R, Boonsirikamchai P, Bhosale P, Marcal L, Faria S, Charnsangavej C. Extramural venous invasion by gastrointestinal malignancies: CT appearances. *Abdom Imaging* 2011; **36**: 491-502 [PMID: 21184063 DOI: 10.1007/s00261-010-9667-8]
- Xu Y, Zhang P, Zhang K, Huang C. The application of CA72-4 in the diagnosis, prognosis, and treatment of gastric cancer. *Biochim Biophys*

- Acta Rev Cancer* 2021; **1876**: 188634 [PMID: 34656687 DOI: 10.1016/j.bbcan.2021.188634]
- 21 **Feng F**, Tian Y, Xu G, Liu Z, Liu S, Zheng G, Guo M, Lian X, Fan D, Zhang H. Diagnostic and prognostic value of CEA, CA19-9, AFP and CA125 for early gastric cancer. *BMC Cancer* 2017; **17**: 737 [PMID: 29121872 DOI: 10.1186/s12885-017-3738-y]
- 22 **He B**, Zhang HQ, Xiong SP, Lu S, Wan YY, Song RF. Changing patterns of Serum CEA and CA199 for Evaluating the Response to First-line Chemotherapy in Patients with Advanced Gastric Adenocarcinoma. *Asian Pac J Cancer Prev* 2015; **16**: 3111-3116 [PMID: 25921105 DOI: 10.7314/apjcp.2015.16.8.3111]
- 23 **Wan Y**, Li Z, Ji N, Gao J. Comparison of gastric vascular anatomy by monochromatic and polychromatic dual-energy spectral computed tomography imaging. *J Int Med Res* 2014; **42**: 26-34 [PMID: 24435514 DOI: 10.1177/0300060513504703]
- 24 **Lv P**, Lin XZ, Chen K, Gao J. Spectral CT in patients with small HCC: investigation of image quality and diagnostic accuracy. *Eur Radiol* 2012; **22**: 2117-2124 [PMID: 22618521 DOI: 10.1007/s00330-012-2485-3]
- 25 **Li J**, Wang Y, Wang R, Gao JB, Qu JR. Spectral CT for preoperative prediction of lymphovascular invasion in resectable gastric cancer: With external prospective validation. *Front Oncol* 2022; **12**: 942425 [PMID: 36267965 DOI: 10.3389/fonc.2022.942425]
- 26 **Matsumoto K**, Jinzaki M, Tanami Y, Ueno A, Yamada M, Kuribayashi S. Virtual monochromatic spectral imaging with fast kilovoltage switching: improved image quality as compared with that obtained with conventional 120-kVp CT. *Radiology* 2011; **259**: 257-262 [PMID: 21330561 DOI: 10.1148/radiol.11100978]



Published by **Baishideng Publishing Group Inc**
7041 Koll Center Parkway, Suite 160, Pleasanton, CA 94566, USA
Telephone: +1-925-3991568
E-mail: office@baishideng.com
Help Desk: <https://www.f6publishing.com/helpdesk>
<https://www.wjgnet.com>

